

Synthesis and Oxygen to Iron Methyl Migration Reaction of the Heterodinuclear Methoxycarbonyne Complex $\text{Cp}(\text{CO})\text{Fe}(\mu\text{-COCH}_3)(\mu\text{-CO})\text{Cr}(\text{CO})(\eta^6\text{-C}_6\text{H}_6)$

Wei Luo, Raymond H. Fong, and William H. Hersh*

Department of Chemistry and Biochemistry, Queens College of the City University of New York, Flushing, New York 11367-1597

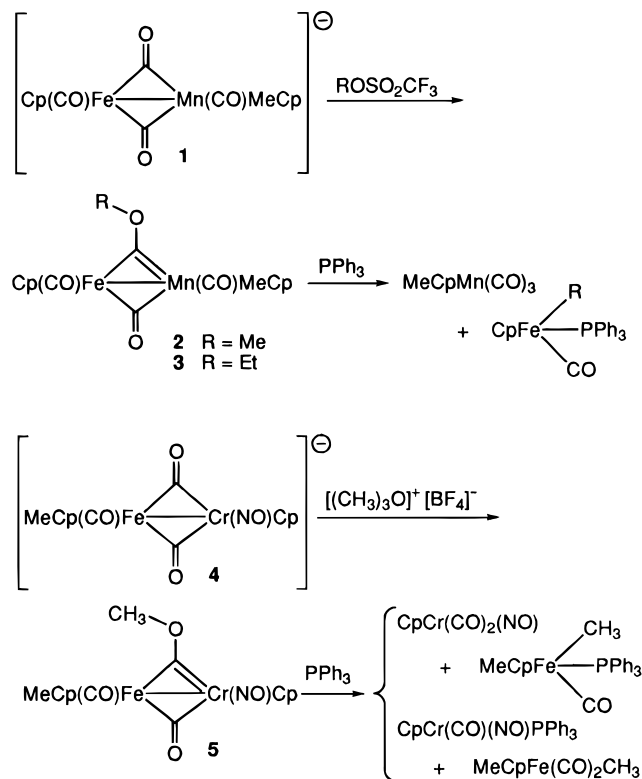
Received May 20, 1997[Ⓢ]

Reaction of $\text{CpFe}(\text{CO})_2\text{-Na}^+\cdot\sim 0.5\text{THF}$ and $(\eta^6\text{-C}_6\text{H}_6)\text{Cr}(\text{CO})_2(\text{CH}_3\text{CN})$ gives the new heterodinuclear anion $\text{Cp}(\text{CO})\text{Fe}(\mu\text{-CO})_2\text{Cr}(\text{CO})(\eta^6\text{-C}_6\text{H}_6)\text{-Na}^+$ (**6-Na⁺**) in 77% yield. Metathesis of **6-Na⁺** with PPN^+Cl^- [PPN^+ = bis(triphenylphosphine)nitrogen(+1)] gives **6-PPN⁺** in 73% yield. Alkylation of **6-Na⁺** was accomplished with $\text{Me}_3\text{O}^+\text{BF}_4^-$ to give the new methoxycarbonyne complex $\text{Cp}(\text{CO})\text{Fe}(\mu\text{-COCH}_3)(\mu\text{-CO})\text{Cr}(\text{CO})(\eta^6\text{-C}_6\text{H}_6)$ (**7**) in 29% yield. Cis/trans isomerization of **6-Na⁺** was observed by ^1H and ^{13}C NMR to occur remarkably rapidly, with $\Delta G^\ddagger(300\text{ K}) = 11.5 \pm 0.6\text{ kcal/mol}$ in CD_3CN . Isomerization of **7** is slower but still rapid by comparison to related compounds, with $\Delta G^\ddagger(300\text{ K}) = 14.3 \pm 1.8\text{ kcal/mol}$ in toluene- d_8 and $15.2 \pm 1.9\text{ kcal/mol}$ in CD_2Cl_2 . Thermal decomposition of **7** provides the fourth example of oxygen to metal methyl migration from a methoxycarbonyne complex. However, it is the first example in which a methoxycarbonyne follows kinetics in which the rate constants are independent of the phosphine concentration, giving $k = 8.1 \pm 0.6 \times 10^{-5}\text{ s}^{-1}$ at 50°C in C_6D_6 for $[\text{PPh}_3] = 0$ to 0.59 M . In the presence of PPh_3 , the products include primarily $(\text{C}_6\text{H}_6)\text{Cr}(\text{CO})_3$ and $\text{CpFe}(\text{CO})(\text{PPh}_3)\text{CH}_3$ but also smaller amounts of $(\text{C}_6\text{H}_6)\text{Cr}(\text{CO})_2\text{PPh}_3$ and $\text{CpFe}(\text{CO})_2\text{CH}_3$. In the absence of PPh_3 , relatively low yields of $(\text{C}_6\text{H}_6)\text{Cr}(\text{CO})_3$ and $\text{CpFe}(\text{CO})_2\text{-CH}_3$ form.

Introduction

We have been studying the chemistry of heteronuclear alkoxycarbonyne complexes for many years since our report of **2**, the first neutral heterodinuclear methoxycarbonyne complex (Scheme 1).^{1–6} This and related compounds are synthesized by alkylation of heterodinuclear anions that have structures analogous to that of the well-known iron dimer $[\text{CpFe}(\text{CO})_2]_2$.^{7,8} That is, each contains two bridging carbonyl ligands, two terminal carbonyl ligands (or one nitrosyl ligand as in **5**), and each compound exists as a mixture of interconverting cis and trans isomers. The carbonynes have the iron dimer structure as well, but with a bridging carbonyne ligand in place of the $\mu\text{-CO}$ ligand. Each carbonyne undergoes a novel thermal decomposition reaction in which the alkyl group migrates from oxygen to iron with concomitant cleavage of the metal–metal bond, as shown for carbonynes **2**, **3**, and **5**. The initially formed iron product in principle could be the 18-electron complex $\text{CpFe}(\text{CO})_2\text{CH}_3$, the unsaturated species $\text{CpFe}(\text{CO})\text{CH}_3$, or more speculatively $\text{CpFe}\equiv\text{COCH}_3$.^{5,9} In practice, the isoelectronic $\text{MeCpMn}(\text{CO})_3$ and CpCr

Scheme 1



$(\text{CO})_2\text{NO}$ molecules are ejected during the thermal decomposition, requiring that $\text{CpFe}(\text{CO})_2\text{CH}_3$ not be a stoichiometrically-formed primary product, and the

[Ⓢ] Abstract published in *Advance ACS Abstracts*, August 15, 1997.
 (1) Fong, R. H.; Hersh, W. H. *Organometallics* **1985**, *4*, 1468–1470.
 (2) Fong, R. H.; Hersh, W. H. *J. Am. Chem. Soc.* **1987**, *109*, 2843–2845.
 (3) Fong, R. H.; Hersh, W. H. *Organometallics* **1988**, *7*, 794–796.
 (4) Fong, R. H.; Lin, C. H.; Idmoumaz, H.; Hersh, W. H. *Organometallics* **1993**, *12*, 503–516.
 (5) Wang, B.; Hersh, W. H.; Rheingold, A. L. *Organometallics* **1993**, *12*, 1319–1330.
 (6) Idmoumaz, H.; Lin, C. H.; Hersh, W. H. *Organometallics* **1995**, *14*, 4051–4063.
 (7) Bryan, R. F.; Greene, P. T. *J. Chem. Soc. A* **1970**, 3064–3068.
 (8) Bryan, R. F.; Greene, P. T.; Newlands, M. J.; Field, D. S. *J. Chem. Soc. A* **1970**, 3068–3074.

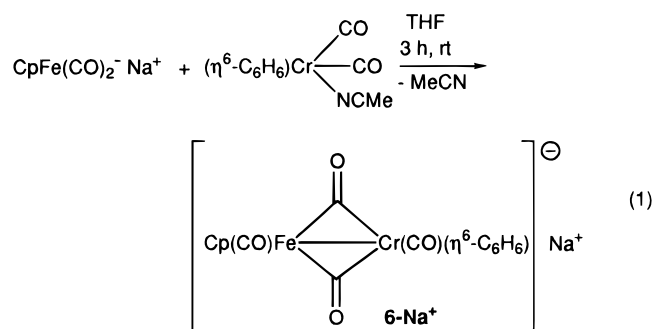
(9) Hersh, W. H. In *Transition Metal Carbonyne Complexes*; F. R. Kreissl, Ed.; Nato ASI Series C: Mathematical and Physical Sciences, Vol. 392; Kluwer Academic Publishers: Dordrecht, 1993; pp 149–150.

alkyl is trapped as $\text{CpFe}(\text{CO})(\text{PPh}_3)\text{R}$ ($\text{R} = \text{Me}, \text{Et}$). In **5** an additional pathway exists in which $\text{CpCr}(\text{CO})\text{NO}$ is ejected and then trapped by external PPh_3 , so here $\text{CpFe}(\text{CO})_2\text{CH}_3$ could form initially. Part of our effort has been directed at trying to understand these details in hopes that light might be shed on the mechanism of the alkyl migration step itself.

In addition to this mechanistic interest, such carbyne chemistry can provide a unique means by which to stitch together metals that might lead to materials with unique nonlinear optical^{10–13} or magnetic properties.^{14–16} Iron and chromium are of special interest for magnetic properties in particular, and for this reason we were particularly interested in iron–chromium carbynes. We report here results on the synthesis and chemistry of a new iron–chromium carbyne in which the $(\eta^6\text{-benzene})\text{-Cr}(\text{CO})$ moiety has been substituted for the $\text{CpCr}(\text{NO})$ moiety of **5**.

Results and Discussion

Synthesis of a Dinuclear Iron–Chromium Anion. A 1:1 molar ratio of solid $\text{CpFe}(\text{CO})_2^-\text{Na}^+ \sim 0.5\text{THF}$ and $(\eta^6\text{-C}_6\text{H}_6)\text{Cr}(\text{CO})_2(\text{CH}_3\text{CN})$ were combined in THF, and the reaction was stirred at room temperature under a nitrogen atmosphere. After 3 h, the reaction was judged to be complete on the basis of monitoring the appearance of a new carbonyl band in the infrared spectrum at 1615 cm^{-1} . Following solvent removal and washing with benzene, the desired anion (**6-Na⁺**) was isolated in 77% yield as a black solid (eq 1). In THF,



the infrared spectrum was complicated by ion-pairing but in acetonitrile it exhibited three strong bands at 1885, 1813, and 1661 cm^{-1} , corresponding to the two terminal and one bridging CO ligands. The room temperature ^1H and ^{13}C NMR spectra of **6-Na⁺** in $\text{CD}_3\text{-CN}$ exhibited one C_6H_6 and one Cp signal, as well as signals indicating the presence of 1.3 equiv of Na^+ -coordinated THF; peaks in the ^{13}C NMR spectrum due to the carbonyl ligands could not be identified (see the variable-temperature NMR section below).

(10) Frazier, C. C.; Harvey, M. A.; Cockerham, M. P.; Hand, H. M.; Chauchard, E. A.; Lee, C. H. *J. Phys. Chem.* **1986**, *90*, 5703–5706.

(11) Tam, W.; Eaton, D. F.; Calabrese, J. C.; Williams, I. D.; Wang, Y.; Anderson, A. G. *Chem. Mater.* **1989**, *1*, 128–140.

(12) Long, N. *J. Angew. Chem., Int. Ed. Engl.* **1995**, *34*, 21–38.

(13) Kanis, D. R.; Ratner, M. A.; Marks, T. J. *J. Am. Chem. Soc.* **1992**, *114*, 10338–10357.

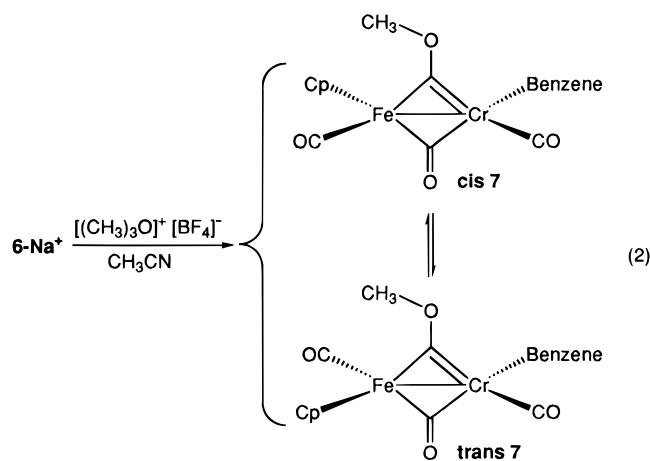
(14) Ziolo, R. F.; Giannelis, E. P.; Weinstein, B. A.; O'Horo, M. P.; Ganguly, B. N.; Mehrotra, V.; Russell, M. W.; Huffman, D. R. *Science* **1992**, *257*, 219–223.

(15) Sunil, D.; Sokolov, J.; Rafailovich, M. H.; Duan, X.; Gafney, H. D. *Inorg. Chem.* **1993**, *32*, 4489–4490.

(16) Strocio, J. A.; Pierce, D. T.; Unguris, J.; Celotta, R. J. *J. Vac. Sci. Technol. B* **1994**, *12*, 1789–1792.

Metathesis of **6-Na⁺** with PPN^+Cl^- [$\text{PPN}^+ = \text{bis}(\text{triphenylphosphine})\text{nitrogen}(+1)$] gave the corresponding **6-PPN⁺** salt. Its IR spectrum in THF simplified to four carbonyl bands at 1894, 1861, 1823, and 1678 cm^{-1} , while in acetonitrile it was virtually identical to that of the sodium salt. The room temperature ^1H NMR spectrum exhibited signals at δ 4.62 (s, 6H) and 4.33 (s, 5H) ppm due to the C_6H_6 and Cp ligands, respectively, and at 7.67–7.44 ppm due to the phenyl protons, while the ^{13}C NMR similarly exhibited signals due to a single set of C_6H_6 , Cp, and PPN^+ carbons; like the Na^+ spectrum, no carbonyl ligands were visible. Integration of the ^1H NMR spectrum consistently gave more phenyl protons than warranted (40% excess under standard acquisition conditions), in part due to long relaxation times of the benzene and cyclopentadienyl ligands. Even increasing the relaxation delay to greater than 20 s did not suffice, but cutting the ^1H flip angle from the usual 30° down to 3° gave constant integrals for 1–20 s relaxation delays. Nevertheless, at best a 10% excess of phenyl protons was still present. Consistent with this, suitable elemental analyses could not be obtained for **6-PPN⁺**, but the low carbon analysis is not consistent with the presence of impurities such as $\text{CpFe}(\text{CO})_2^-\text{PPN}^+$ or PPN^+Cl^- which have the requisite extra phenyl protons but are higher rather than lower in the percentage of carbon. Both **6-PPN⁺** and **6-Na⁺** were found to be unstable in methylene chloride, so this solvent could not be used for recrystallization and further purification could not be accomplished. Interestingly, **4-PPN⁺** was also found to be unstable in methylene chloride.

Synthesis of an Iron–Chromium Methoxycarbene. Alkylation of the heterodinuclear anion was carried out by rapid addition of 1 equiv of $(\text{CH}_3)_3\text{O}^+\text{BF}_4^-$ to a CH_3CN solution of **6-Na⁺**; after 5 min of stirring followed by solvent removal, the desired carbyne **7** was obtained as a brown solid that was contaminated by substantial amounts of $[\text{CpFe}(\text{CO})_2]_2$ and $(\text{C}_6\text{H}_6)\text{Cr}(\text{CO})_3$ (eq 2). Purification by chromatography could not be



carried out due to decomposition of the carbyne product on the column. Nonetheless, subsequent workup followed by two recrystallizations from $\text{CH}_2\text{Cl}_2/\text{hexane}$ gave a spectroscopically pure material. Similar to the anion **6-PPN⁺**, a suitable elemental analysis could not be obtained, although in this case the cause is undoubtedly due to the thermal instability of the carbyne. The overall yield after the two recrystallizations was 29%.

Table 1. Infrared Stretching Frequencies in Dinuclear [CpFe(CO)₂]₂ Analogs

cmpd (solvent)	Fe–CO	M'–CO	μ-CO	Cr–NO
1-PPN⁺ (CH ₂ Cl ₂)	1899	1832	1671	
4-PPN⁺ (CH ₃ CN)	1891		1698	1588
6-PPN⁺ (CH ₃ CN)	1886	1812	1661	
[CpFe(CO) ₂] ₂ (CH ₂ Cl ₂)	1996	1954	1773	
2 (THF)	1954	1907	1774	
<i>cis</i> - 5 (C ₆ H ₆)	1966		1794	1659
7 (CH ₂ Cl ₂)	1943	1876	1736	

While this is significantly lower than that obtained for iron–manganese carbynes **2** and **3**, it is higher than that obtained for the iron–chromium carbyne **5**. This effect presumably is due to the higher nucleophilicity of the bridging CO ligands in the non-nitrosyl anion **6**, as reflected in the lower CO stretching frequencies (see below).

The IR spectrum of **7** exhibits strong bands at 1943 and 1876 cm⁻¹ for the two terminal CO ligands and one strong band at 1736 cm⁻¹ for the bridging carbonyl. These bands are consistent with retention of the iron dimer type structure and absence of the negative charge (see below).

Both the ¹H and ¹³C NMR spectra clearly exhibit broad lines due to a dynamic process as indicated in eq 2. The room temperature ¹H NMR spectrum in C₆D₆ for instance was not particularly informative, consisting of broad peaks at 4.56 and 4.41 ppm due to the overlapping and interconverting cyclopentadienyl and benzene ligands and a sharp peak at 4.25 ppm due to the methoxy group. In CD₂Cl₂, a broad but more informative spectrum was obtained, exhibiting peaks at 5.32, 4.87, and 4.66 ppm that on the basis of relative integrals are due to the benzene, methoxy, and Cp ligands, respectively. The room temperature ¹³C NMR spectrum (CD₂Cl₂) exhibited a peak at 392.2 ppm that is typical of μ-carbyne resonances; for instance, that in **2** is at 391 ppm and that in **5** is at 428 ppm.^{4,5} The methyl from the alkylating reagent is clearly incorporated as a methoxy group, as judged by the new methoxy signal at 71.5 ppm. In addition, signals indicative of two terminal CO ligands (236.7 ppm, Cr–CO; 215.0 ppm, Fe–CO) and one bridging CO (285.2 ppm) were observed. Two broad peaks were observed for the Cp and benzene peaks at 85.77 and 97.39 ppm, respectively, but in addition, two much smaller broad peaks at 98.84 and 88.05 ppm suggested the presence of a second isomer in a 75:25 ratio. The intensities of the other bands were too small to allow peaks for the second isomer to be observed above the noise, with the exception of the methoxy peak, but presumably methoxy peaks for the two isomers overlap as observed previously.⁴

Infrared Spectra of Iron Dimer Analogs. Infrared data are collected in Table 1 for the heterodinuclear anions and carbynes that have been discussed above, along with that of the iron dimer [CpFe(CO)₂]₂. The carbonyl bands of **6-PPN⁺** are each about 10–20 cm⁻¹ lower than those of **1-PPN⁺**, and the value for the bridging CO ligands in **6-PPN⁺** is nearly 40 cm⁻¹ lower than that for **4-PPN⁺**. The lower CO stretching frequencies indicate the presence of more negative charge on these ligands. Presumably, the strongly π-acidic NO ligand in **4-PPN⁺** removes electron density from the bridging CO ligands more than the terminal CrCO ligand does in **6-PPN⁺**, and the neutral benzene ligand

of **6** permits a lower oxidation state than the anionic Cp⁻ ligand of **1** and **4** does. The bands of **6-PPN⁺** are all lower than those of the isoelectronic and isostructural iron dimer [CpFe(CO)₂]₂ by >100 cm⁻¹ due to the negative charge; those at 1885 and 1661 cm⁻¹ are ~110 cm⁻¹ lower than those in the iron dimer at 1996 and 1773 cm⁻¹, while the third band is ~140 cm⁻¹ lower than that in the iron dimer at 1954 cm⁻¹ and, therefore, may be due to the CrCO ligand.

All of the terminal carbonyl ligands exhibit lower frequencies in the carbynes than those seen in the iron dimer, so it is reasonable to conclude that the carbyne ligand is not as electron-withdrawing as a bridging carbonyl ligand. The remaining bridging carbonyl ligand in **2** has the same frequency as the μ-CO of the iron dimer while that in **5** is higher. In contrast, the bridging carbonyl ligand in **7** is much lower in frequency, as is the terminal carbonyl ligand on Cr at 1876 cm⁻¹. Here, once again then, the (η⁶-C₆H₆)Cr fragment appears to be more electron-rich than the MeCpMn or CpCr(NO) fragments.

Variable-Temperature NMR Spectra of Anion 6-Na⁺ and Methoxycarbyne 7. While the purity of the PPN⁺ salt of **6** is higher than that of the Na⁺ salt, the solubility is much lower and suitable ¹³C NMR spectra could not be obtained. The Na⁺ salt, as judged from the IR spectrum in acetonitrile, is not ion-paired, so except for the question of purity it would be expected to give useful spectra of the heterodinuclear anion. At room temperature, both salts gave a single peak for each of the benzene and cyclopentadienyl moieties in the ¹H and ¹³C NMR spectra as described above. Upon cooling **6-Na⁺** to -50 °C, each singlet split into two broad singlets in a 63:37 ratio, consistent with the presence of interconverting *cis* and *trans* isomers, as previously observed for the Fe–Mn anion.⁴ Spectra were simulated using the chemical shifts and isomer ratios at -50 °C, giving in the ¹³C NMR (for *cis* to *trans* isomerization) $k_{ct} = 12 \pm 2 \text{ s}^{-1}$ at -50 °C but requiring $k_{ct} \geq 15\,000 \text{ s}^{-1}$ at 22 °C to fit the coalesced spectrum. A lower rate suffices to simulate the room temperature ¹H NMR spectrum, where coalescence occurs by -20 °C at $k_{ct} = 500 \pm 50 \text{ s}^{-1}$, but there is no difference in the simulated spectra at 22 °C for $k_{ct} \geq 5000 \text{ s}^{-1}$ since the fast-exchange limit has already been reached. A linear plot of $\ln(k_{ct}/T)$ vs $1/T$ was obtained, giving $\Delta G^\ddagger(300 \text{ K}) = 11.5 \pm 0.6 \text{ kcal/mol}$, $\Delta H^\ddagger = 12.6 \pm 0.3 \text{ kcal/mol}$, and $\Delta S^\ddagger = 3.7 \pm 1.4 \text{ eu}$. By comparison, the rate constant for **1-PPN⁺** in CD₂Cl₂ at 297 K was $14 \pm 1 \text{ s}^{-1}$, with $\Delta G^\ddagger(300 \text{ K}) = 15.8 \pm 0.4 \text{ kcal/mol}$. The barrier for *cis/trans* isomerization of **6-Na⁺** is remarkable in that it is the lowest we know of for a compound of the iron dimer structure. The next lowest is [CpFe(CO)₂]₂ itself, for which $\Delta G^\ddagger(220 \text{ K}) \approx 12 \text{ kcal/mol}$. While we can only speculate as to the cause, it is possible that the Na⁺ ion is responsible rather than some intrinsic property of the organometallic anion. Finally, bands for only a single set of bridging and terminal CO ligands were observed in the ¹³C NMR spectrum at -50 °C, which we presume are due to the *cis* isomer alone. The *trans* isomer, as proposed previously,^{4,17,18} allows rapid interconversion of the bridging and terminal CO ligands,

(17) Adams, R. D.; Cotton, F. A. *J. Am. Chem. Soc.* **1973**, *95*, 6589–6594.

(18) Farrugia, L. J.; Mustoo, L. *Organometallics* **1992**, *11*, 2941–2944.

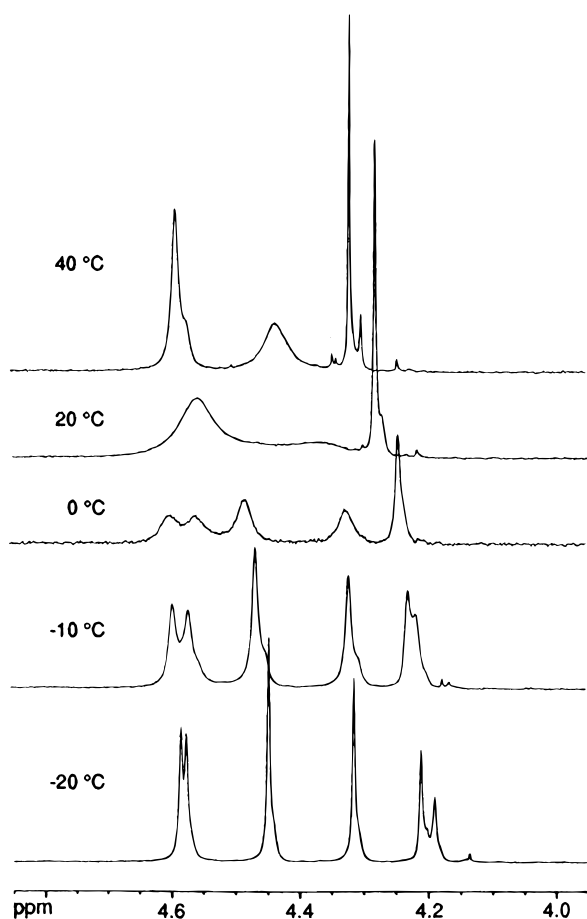


Figure 1. Variable-temperature ^1H NMR spectra (400 MHz) of **7** in toluene- d_8 .

hence preventing their observation despite the absence of cis–trans isomerization.

The spectra of methoxycarbene **7** were the most straightforward in CD_2Cl_2 , as described above, so we start here. Cooling to $-20\text{ }^\circ\text{C}$ gives a simple ^1H NMR spectrum consistent with the presence of two isomers in a 82:18 ratio; each of the benzene, methoxy, and cyclopentadienyl signals is split into two bands. In the ^{13}C NMR, a similar cis–trans ratio was observed for the benzene and Cp bands as well as the terminal CO peaks. At this temperature, the peaks are quite sharp and separate bands for the cis and trans isomers were observed for all carbons, except the bridging carbonyl and carbene (including the methoxy) ligands; the intensities of the peaks due to the bridging carbon atoms were low, however, and the isomer peaks could be below the noise level. Carbynes **2** and **5** exhibited resolved peaks (typical $\Delta\nu \approx 1$ ppm) for most carbons in the two isomers, the exceptions being the methoxy carbon and terminal FeCO in **2**. Spectra were simulated using both the chemical shifts and isomer ratios in the ^1H and ^{13}C NMR spectra at $-20\text{ }^\circ\text{C}$, and in sharp contrast to anion **6**, $k_{\text{ct}} < 1\text{ s}^{-1}$ at $-20\text{ }^\circ\text{C}$ and less than 55 s^{-1} at $22\text{ }^\circ\text{C}$, where the ^1H NMR peaks are past coalescence but the ^{13}C peaks are resolved albeit still broadened.

The room temperature ^1H NMR spectra in toluene- d_8 were virtually identical to those in C_6D_6 described above. As seen in Figure 1, cooling results in decoalescence of both the very broad band just downfield of the sharp methoxy resonance as well as the large broad downfield peak to give four new bands at $0\text{ }^\circ\text{C}$; by -10

$^\circ\text{C}$, even the methoxy peak begins to be resolved into two bands. Integration of the $-20\text{ }^\circ\text{C}$ spectrum is consistent with assignment of the bands at 4.2 ppm to the methoxy peaks of the two isomers, the bands at 4.45 and 4.32 to the benzene and Cp peaks of the major isomer, and the two downfield bands to those of the minor isomer. The variable-temperature spectra were simulated using the temperature-dependent integrated isomer ratios and chemical shifts. Without the latter in particular, the spectra could not be fit, and near perfect linear correlations of chemical shifts with the three lowest temperatures were observed, allowing simple extrapolation. Assignment of the downfield peak at 4.59 ppm as a benzene rather than a Cp peak was made initially on the basis of height, but while line shape analysis shows this is not justified on this basis alone, it is the only assignment that correctly fits the temperature-dependent chemical shifts. No other assignment, other than switching the identities of the peaks at 4.59 and 4.58 ppm, allowed the broad spectra to be simulated. Warming above room temperature sharpens the three bands, and data were collected even at $40\text{ }^\circ\text{C}$ without significant thermal decomposition.

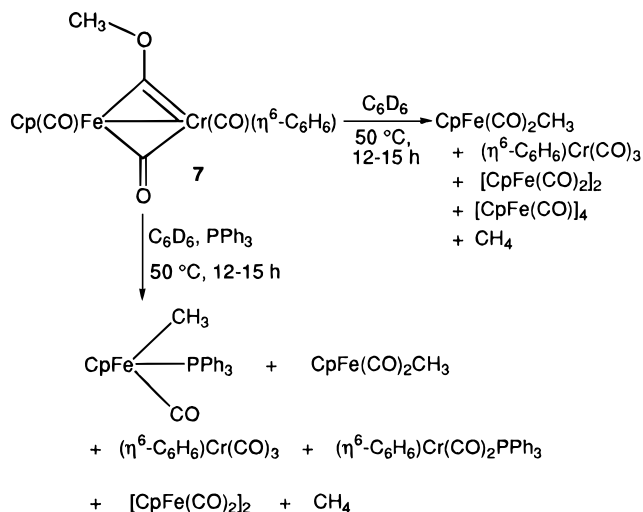
The derived barrier for cis/trans isomerization of **7** is $\Delta G^\ddagger(300\text{ K}) = 14.3 \pm 1.8$ kcal/mol in toluene- d_8 and $\Delta G^\ddagger(300\text{ K}) = 15.2 \pm 1.9$ in CD_2Cl_2 . Direct inspection of the rate constants suggests the difference is statistically significant; for instance, in CD_2Cl_2 $k_{\text{ct}} = 0.6 \pm 0.4$ and $25 \pm 5\text{ s}^{-1}$ at -20 and $+22\text{ }^\circ\text{C}$ in the ^1H NMR, while in toluene- d_8 $k_{\text{ct}} = 2.0 \pm 0.5$ and $180 \pm 40\text{ s}^{-1}$ at -20 and $+20\text{ }^\circ\text{C}$. For carbene **2**, $\Delta G^\ddagger(300\text{ K}) = 16.4 \pm 0.7$ kcal/mol, while carbene **5** did not undergo exchange at a measurable rate and the cis and trans isomers were chromatographically separated.⁵ As noted above, all compounds with the iron dimer structure have higher barriers than that seen in **6-Na**⁺ and most have higher barriers than **7** as well. It is reasonable to assume, therefore, that the low barrier for **6-Na**⁺ is at least in part a reflection of its structure rather than an artifact of the particular solvent and cation present. It is possible that the relatively electron-rich nature of **6-Na**⁺ and **7** is in some way responsible for the low barriers, but further speculation is unwarranted.

The identity of the major isomer in both **6** and **7** cannot be determined with certainty. Since methylene chloride (dielectric constant = 9.1) is more polar than toluene (dielectric constant = 2.38), the simplest hypothesis^{4,19,20} is that the cis isomer is favored in both methylene chloride (82:18 cis/trans ratio at $-20\text{ }^\circ\text{C}$) and toluene (59:41 cis/trans ratio at $-20\text{ }^\circ\text{C}$); alternatively, the lower polarity of toluene could lead to a crossover of isomer stability and the trans isomer could be dominant. However, integration of the toluene- d_8 ^1H NMR spectra shows that as the temperature is increased, so is the relative ratio of the minor isomer (i.e., 52:48 cis:trans at $0\text{ }^\circ\text{C}$), consistent with it being the thermodynamically disfavored trans isomer. Similar ratios were seen for **2** at room temperature in methylene chloride (74:26) and benzene (68:32), although no variation in the cis–trans ratio was observed over a temperature range comparable to that used here.⁴ The 63:37 isomer ratio observed for **6-Na**⁺ in acetonitrile at -50

(19) Bullitt, J. G.; Cotton, F. A.; Marks, T. J. *Inorg. Chem.* **1972**, *11*, 671–676.

(20) Kirchner, R. M.; Marks, T. J.; Kristoff, J. S.; Ibers, J. A. *J. Am. Chem. Soc.* **1973**, *95*, 6602–6613.

Scheme 2

Table 2. Yield (%) and Rate Constant Data for the Thermal Decomposition of 7^a

product	[PPh ₃]			
	0	0.19	0.38	0.59
(C ₆ H ₆)Cr(CO) ₃	38	55	55	72
(C ₆ H ₆)Cr-(CO) ₂ (PPh ₃)		14	20	12
CpFe(CO) ₂ (CH ₃)	18	7	10	11
CpFe(CO)-(PPh ₃)(CH ₃)		35	41	36
[CpFe(CO) ₂] ₂	8	16	10	6
[CpFe(CO) ₂] ₄	4	0	0	0
CH ₄	2	2	3	3
total Cr	38	70	75	83
total Fe	30	58	61	52
rate constant ^b	8.66 ± 0.39	8.47 ± 0.15	7.09 ± 0.09	8.00 ± 0.16

^a Concentrations of **7** for the four runs were 0.015, 0.026, 0.0110, and 0.0112 M. ^b First-order rate constant for the decomposition of **7** at 50.4 ± 0.1 °C in C₆D₆, × 10⁵ s⁻¹.

°C does not shed any light on the identity of the isomers; previous work with the PPN⁺ and Ph₃PMe⁺ salts of **1** and **4** showed these ratios to be both cation and temperature dependent.^{4,5}

Thermal Decomposition of Methoxycarbyne 7. Heating carbyne **7** in a sealed NMR tube in benzene-*d*₆ at 50 °C resulted in complete decomposition in 15 h in both the absence and presence of PPh₃. The reactions are shown in Scheme 2, and the product data and rate constants are collected in Table 2. Products were identified by comparison of the ¹H, ¹³C, and ³¹P NMR chemical shifts to those of authentic samples; details may be found in the Experimental Section.

The qualitative results of the decomposition of **7** are similar to those previously observed for **2**, **3**, and **5**. The key result is that, once again, oxygen to iron methyl migration is observed, with concomitant bond cleavage to give mononuclear products. In the absence of PPh₃, large amounts of a black precipitate form since the system is deficient in donor ligand; decomposition releases CO, presumably, which is scavenged by the remaining products. The yield of (benzene)Cr(CO)₃ is the highest, which suggests that chromium is either more effective in scavenging CO or that it is the kinetic product of the methyl migration and Fe–Cr bond cleavage. This would then yield CpFe(CO)CH₃, which could scavenge CO to give a low yield of CpFe(CO)₂CH₃, lose the methyl radical to give the cluster [CpFe(CO)]₄,

or do both to give the iron dimer [CpFe(CO)₂]₂; consistent with this, low yields of methane were observed.

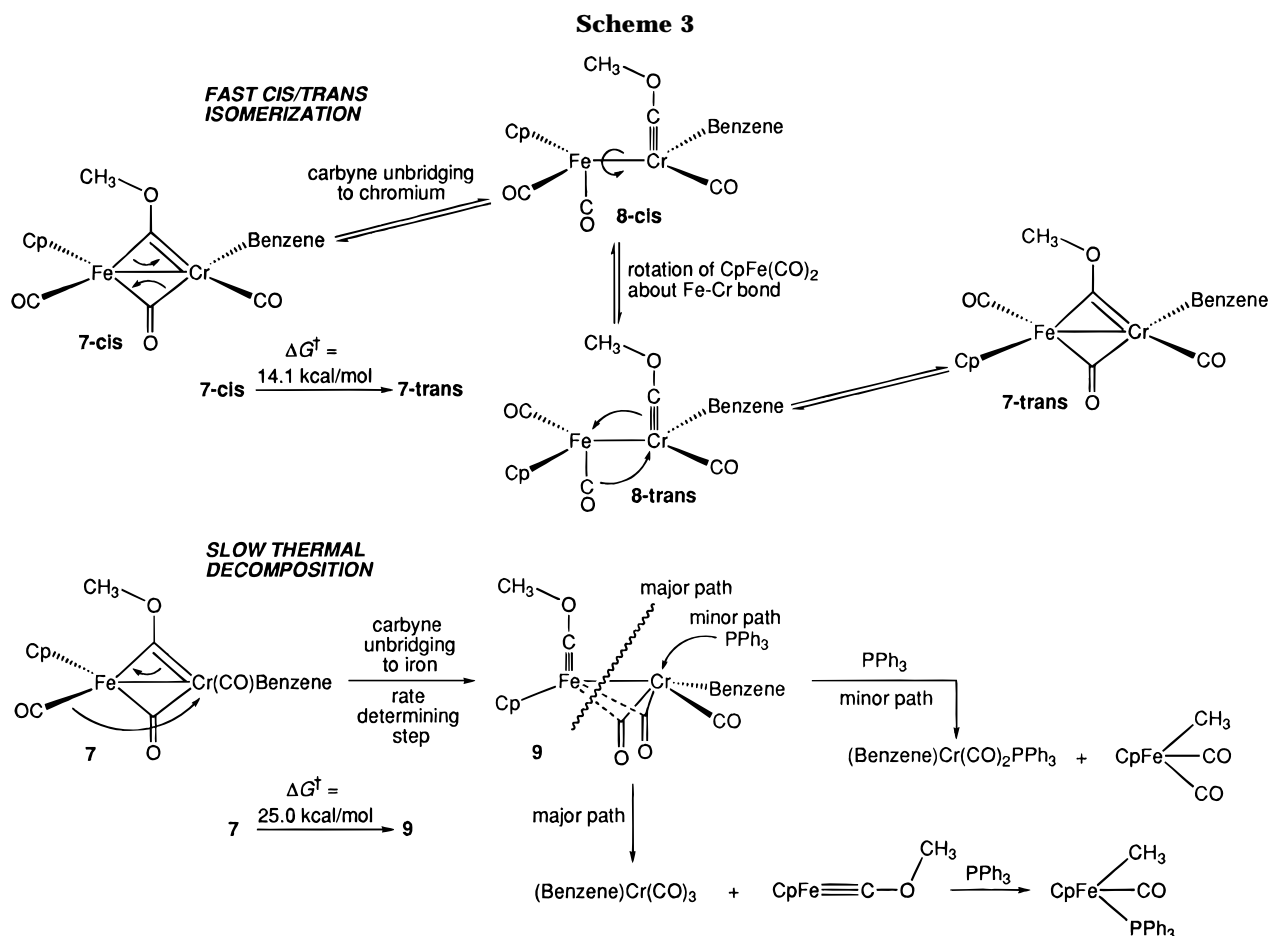
In the presence of PPh₃, a stoichiometric reaction to give (benzene)Cr(CO)₃ and CpFe(CO)(PPh₃)CH₃ is possible, but chromium products still form in higher yield than do the iron products. Indeed, formation of both (benzene)Cr(CO)₃ and a smaller amount of (benzene)Cr(CO)₂PPh₃ suggests the presence of one reaction pathway that ejects (benzene)Cr(CO)₃ from the carbyne and one that ejects (benzene)Cr(CO)₂ which is then trapped by PPh₃. Under the reaction conditions, preformed (benzene)Cr(CO)₃ would react with PPh₃ to give (benzene)Cr(CO)₂PPh₃, but in less than 10% yield. Actual yields (based on total chromium) of 14–27% show that a pathway for the formation of (benzene)Cr(CO)₂PPh₃ from carbyne **7** must exist, but the difference is small. The two pathways were observed for iron–chromium carbynes **2** and **3**, where only MeCpMn(CO)₃ and CpFe(CO)(PPh₃)R formed. In the case of the iron adduct, CpFe(CO)(PPh₃)CH₃ would not be expected to form from CpFe(CO)₂CH₃ and PPh₃ under the reaction conditions.²¹

The rates of the decomposition reactions were followed in order to determine their dependence (if any) on PPh₃. Within experimental error, the rate of decomposition of **7** is first order and independent of [PPh₃], averaging (8.1 ± 0.6) × 10⁻⁵ s⁻¹ over a range of phosphine concentration from 0 to 0.59 M. Previously, the only instance of this behavior was exhibited by ethoxycarbyne **3**. Both **2** and **5** exhibited phosphine-dependent pathways to give a different product, namely the MePPh₃⁺ salt of the initial dinuclear anion via dealkylation of the carbyne by PPh₃. Consistent with this absence of rate dependence on [PPh₃], very little precipitate was observed in the PPh₃ reactions of **7**, unlike those with **2** and **5**, and isolation of the small amount of residue confirmed that it was not **6-PPh₃Me**⁺ nor any other Cp or benzene containing material. As noted repeatedly above, the IR data is consistent with **6-PPN**⁺ being relatively electron-rich, so this phosphine-induced dealkylation route may be inhibited.

The major mystery in the data collected is that as the phosphine concentration increases, the ratio of CpFe(CO)(PPh₃)CH₃ to CpFe(CO)₂CH₃ decreases rather than increases as might be expected. It is important to assess the certainty of this trend. While it is clear that the ratio goes roughly from 5 to 4 to 3 as [PPh₃] goes from 0.19 to 0.38 to 0.59 M, examination of the percent yields might suggest that this ratio is an artifact, since both the CpFe(CO)₂CH₃ and CpFe(CO)(PPh₃)CH₃ yields vary little (from 7 to 11% for the former and from 35 to 41% for the latter). However, direct examination of the spectra clearly shows that the trend is real, both by comparison of the ratio of the Cp peaks and in the methyl region where CpFe(CO)₂CH₃ gives a singlet in the midst of the CpFe(CO)(PPh₃)CH₃ doublet in the high [PPh₃] runs but is buried in the low [PPh₃] run.

Mechanistic Proposals. A mechanism that is consistent with the results described here and previously is shown in Scheme 3. Three key experimental observations are incorporated into this mechanism. First, **7** undergoes cis/trans isomerization; at 50 °C, the calculated rate constant *k*_{ct} ≈ 1900 s⁻¹ and the activation

(21) Su, S. R.; Wojcicki, A. *J. Organomet. Chem.* **1971**, *27*, 231–240.



barrier $\Delta G_{\text{ct}}^\ddagger(50^\circ\text{C}) = 14.1 \pm 1.9 \text{ kcal/mol}$. The calculated cis:trans ratio is 45:55 at this temperature, with a corresponding thermodynamic energy difference of less than 0.3 kcal/mol. Second, the rate of decomposition of **7** is first-order and independent of phosphine concentration, with $k_{\text{dec}} = (8.1 \pm 0.6) \times 10^{-5} \text{ s}^{-1}$ giving an activation barrier $\Delta G_{\text{dec}}^\ddagger(50^\circ\text{C}) = 25.0 \pm 0.1 \text{ kcal/mol}$. Third, the ratio of $\text{CpFe}(\text{CO})(\text{PPh}_3)\text{CH}_3$ to $\text{CpFe}(\text{CO})_2\text{CH}_3$ decreases as $[\text{PPh}_3]$ increases. As will be described below, these facts are best accounted for by the presence of two intermediates, one a low-energy intermediate involved in cis/trans isomerization and the other a high-energy intermediate formed from **7** which gives rise to products in subsequent non-rate-determining steps.

Cis/trans isomerization of $[\text{CpFe}(\text{CO})_2]_2$ has been proposed to proceed via the unbridged intermediate $\text{Cp}(\text{CO})_2\text{Fe}-\text{Fe}(\text{CO})_2\text{Cp}$,¹⁸ and a wide variety of iron dimer analogs with non-carbonyl bridges undergoes such isomerization at comparable rates.⁴ The simplest assumption is that all of these isomerizations proceed via the same mechanism, so if this is assumed to be the case for **7** as well, then an iron–chromium single-bonded intermediate must be present. Unlike the iron dimer case, however, unbridging of the carbyne ligand of **7** to either metal should have different energy barriers and can have different stereochemical outcomes as well. We have previously proposed that cis–trans isomerization occurs via unbridging of the carbyne to a single metal, since only in this way is NMR-exchange of diastereotopic protons (when present) prevented.⁴ Here, we propose exclusive carbyne unbridging to chromium to give

intermediate **8**, as shown in Scheme 3, since only in this way can an intermediate form that incorporates two 18-electron metal centers. The activation energy is roughly comparable to that seen in the iron dimer, and one might suppose that unbridging to iron to give formally 19-electron iron and 17-electron chromium centers would be disfavored. Of course, the 14 kcal/mol barrier to cis/trans isomerization includes rotation about the metal–metal bond as well as unbridging, so one cannot dismiss the possibility that unbridging to both metals occurs but that the 17-electron/19-electron intermediate simply does not undergo bond rotation.

Under the reaction conditions, cis/trans isomerization is rapid and similar amounts of each isomer are present, and we presume that thermal decomposition of **7** occurs from both isomers. Since PPh_3 is incorporated in the products without involvement in the rate-determining step, an intermediate having a barrier to its formation of the full 25 kcal/mol is required. We propose that carbyne unbridging to iron with concomitant CO bridging occurs to give **9**. The structure is proposed based on analogy to known semibridged heterodinuclear compounds^{22–25} and presumably is higher in energy than **8** due to the 17/19-electron imbalance, even though it is ameliorated by the presence of semibridging carbonyl ligands.

(22) Leonhard, K.; Werner, H. *Angew. Chem., Int. Ed. Engl.* **1977**, *16*, 649–650.

(23) Werner, H.; Juthani, B. *J. Organomet. Chem.* **1981**, *209*, 211–218.

(24) Werner, H. *Pure Appl. Chem.* **1982**, *54*, 177–188.

(25) Aldridge, M. L.; Green, M.; Howard, J. A. K.; Pain, G. N.; Porter, S. J.; Stone, F. G. A.; Woodward, P. *J. Chem. Soc., Dalton Trans.* **1982**, 1333–1340.

The third experimental observation noted above requires a partitioning of the carbyne decomposition into two pathways *after* the phosphine-independent rate-determining step, and so an irreversibly-formed intermediate must be involved. In the absence of phosphine, the major pathway leads to (benzene)Cr(CO)₃ and the proposed iron carbyne intermediate CpFe≡COCH₃.^{5,9} This iron species is electron-deficient and must abstract CO in order to yield CpFe(CO)₂CH₃. Some of this CO must ultimately come from the (benzene)Cr(CO)₃, and so its yield is somewhat lower in the absence of PPh₃ than in the three runs in which PPh₃ is added. The key point is that the minor pathway requires trapping of intermediate **9** by PPh₃ to give the *alternate* pair of products, which includes CpFe(CO)₂CH₃. At high phosphine concentration, relatively more of these minor products should form, leading to the counterintuitive result that more CpFe(CO)₂CH₃ relative to CpFe(CO)(PPh₃)CH₃ forms at higher phosphine concentrations. As an alternative mechanism, one might suppose that the 25 kcal/mol step leads directly to metal–metal bond cleavage to give (benzene)Cr(CO)₃ and CpFe≡COCH₃ or (benzene)Cr(CO)₂ and CpFe(CO)₂CH₃. If this were the case, however, there likely would be no dependence of product ratios on PPh₃ concentration. We have previously described kinetic evidence in the thermal decomposition of carbyne **5** that similarly is best accounted for by the presence of a metal–metal bonded intermediate analogous to **9**.⁵

The mechanism involving **9** should have two other consequences: similar amounts of (benzene)Cr(CO)₂PPh₃ and CpFe(CO)₂CH₃ should form and less (benzene)Cr(CO)₃ should form at higher phosphine concentrations. The first consequence is very roughly observed; about half as much CpFe(CO)₂CH₃ as (benzene)Cr(CO)₂PPh₃ forms, although some of the excess chromium adduct could arise from direct thermal reaction of (benzene)Cr(CO)₃ with PPh₃. At present, we have no explanation for the failure to account for the second consequence.

The actual rate of decomposition of **7** may be compared to the first-order, phosphine-independent pathways observed for the other carbynes: $1.0 \times 10^{-4} \text{ s}^{-1}$ at 75 °C for **2**, $1.0 \times 10^{-4} \text{ s}^{-1}$ at 65 °C for **3**, and $6.5 \times 10^{-4} \text{ s}^{-1}$ at 50 °C for **5**. The rate of $8 \times 10^{-5} \text{ s}^{-1}$ for **7** at 50 °C is nearly the same as those for the iron–manganese carbynes **2** and **3** but at higher temperatures and is an order of magnitude slower than that of the iron–chromium carbyne **5** at the same temperature. These rates can be converted to activation energies to give a better, albeit still rough, guide to relative reactivity: at the reaction temperatures noted above, $\Delta G^\ddagger = 23.7 \text{ kcal/mol}$ for **5**, 25.0 kcal/mol for **7**, 26.1 kcal/mol for **3**, and 26.8 kcal/mol for **2**. Clearly, the isoelectronic fragments that make up the non-iron portion of these carbynes can be ranked in order of the stability they impart as MeCpMn(CO) > (benzene)Cr(CO) > CpCr(NO). While the differences are modest, they are experimentally significant: we would predict, for instance, that the ethoxycarbyne analog of **5** would be difficult to isolate, and the larger array of products and apparent intermediates observed in the decomposition of **5** and **7** is due to their greater reactivity.

In conclusion, the experimental observations for the current study as well as those previously described are most readily explained by the presence of different

barriers to carbyne unbridging to either metal. One of the resultant energetically different intermediates is involved in cis–trans isomerization, the other in thermal decomposition. Phosphine attack with concomitant metal–metal bond cleavage can occur on the high-energy decomposition intermediate competitive with phosphine-independent fragmentation. The details of the novel methyl migration reaction itself remain unknown.

Experimental Section

General Considerations. All manipulations of air-sensitive compounds were carried out in a Vacuum Atmospheres inert-atmosphere drybox under recirculating nitrogen. NMR spectra were recorded on a Bruker DPX-400 spectrometer; chemical shifts are reported relative to residual hydrogen in C₆D₆ (δ 7.15), CD₂Cl₂ (δ 5.32), CD₃CN (δ 1.93), C₆D₅CD₃ (δ 2.09), and to carbon in C₆D₆ at 128.0 ppm, CD₂Cl₂ at 53.8 ppm, or CD₃CN at 1.3 ppm. NMR line-shape analyses were carried out using gNMR (Cherwell Scientific Publishing, Inc.) on a Macintosh computer. Infrared spectra were obtained on a Mattson Galaxy 4020 FT-IR. Elemental analyses were performed by Desert Analytics, Tucson, AZ.

All solvents were treated under nitrogen. Acetonitrile was purified by sequential distillation from calcium hydride and phosphorus pentoxide. Benzene and tetrahydrofuran were distilled from sodium benzophenone ketyl. Hexane was purified by washing successively with 5% nitric acid in sulfuric acid, water, sodium bicarbonate solution, and water and then dried over calcium chloride and distilled from *n*-butyllithium in hexane. Methylene chloride was distilled from phosphorus pentoxide; CD₂Cl₂ was vacuum-transferred from phosphorus pentoxide. CD₃CN was dried over 4-Å molecular sieves and vacuum-transferred prior to use; benzene-*d*₆ and toluene-*d*₈ were vacuum-transferred from sodium benzophenone ketyl.

Celite was dried in an oven at 140 °C overnight prior to use. Trimethylxonium tetrafluoroborate (Lancaster Synthesis) was used as received. CpFe(CO)₂[−]Na⁺·0.5THF,⁴ CpFe(CO)(PPh₃)(CH₃),^{4,21,26} (C₆H₆)Cr(CO)₂(CH₃CN),²⁷ (C₆H₆)Cr(CO)₂(PPh₃),²⁸ (C₆H₆)Cr(CO)₃,²⁹ and PPN⁺Cl[−]³⁰ were prepared according to published procedures.

[Cp(CO)Fe(μ -CO)₂Cr(CO)(C₆H₆)][−]Na⁺ (6-Na⁺**).** To a mixture of solid CpFe(CO)₂[−]Na⁺·0.5THF (0.951 g, 4.03 mmol) and (C₆H₆)Cr(CO)₂(CH₃CN) (0.961 g, 4.23 mmol) was added 100 mL of THF. The solution was stirred at room temperature for 3 h and filtered through Celite, and the solvent was removed on a vacuum line. The resultant black solid was purified by stirring for a few minutes with benzene, filtering, and then washing several times with 5-mL portions of benzene until these washes were nearly colorless, yielding 1.48 g (77% yield based on Fe and the presence of 1.3 equiv THF by ¹H NMR (CD₃CN)) of product as a black solid. IR (THF): 1968 (w), 1902 (m), 1889 (m), 1833 (m), 1709 (w), 1615 (br, m) cm^{−1}. IR (CH₃CN): 2018 (w), 1964 (w), 1885(s), 1813 (m), 1661 (s) cm^{−1}. ¹H NMR (CD₃CN, 27 °C): δ 4.64 (s, 6H), 4.34 (s, 5H), 3.63, 1.79 (THF). ¹H NMR (CD₃CN, −50 °C): δ 4.76, 4.67 (C₆H₆, 63:37 cis:trans), 4.42, 4.29 (Cp, 63:37 cis:trans). ¹³C NMR (CD₃CN, 27 °C): δ 93.42 (C₆H₆), 86.86 (Cp), 68.27, 26.19 (THF). ¹³C NMR (CD₃CN, −50 °C): δ 311.63 (μ -CO), 242.72 (CrCO), 217.85 (FeCO), 94.04 (C₆H₆, trans), 92.50 (C₆H₆, cis), 87.71 (Cp, trans), 85.58 (Cp, cis), 67.81, 25.76 (THF) ppm.

[Cp(CO)Fe(μ -CO)₂Cr(CO)(C₆H₆)][−]PPN⁺ (6-PPN⁺**).** To a mixture of 0.200 g (0.417 mmol) of **6-Na⁺**·1.3THF and 0.239 g

(26) Treichel, P. M.; Shubkin, R. L.; Barnett, K. W.; Reichard, D. *Inorg. Chem.* **1966**, *5*, 1177–1181.

(27) Knoll, L.; Reiss, K.; Schäfer, J.; Klüfers, P. *J. Organomet. Chem.* **1980**, *193*, C40–C42.

(28) Strohmeier, W.; Hellmann, H. *Chem. Ber.* **1963**, *96*, 2859–2866.

(29) Mahaffy, C. A. L.; Pauson, P. L. *Inorg. Synth.* **1990**, *28*, 136–140.

(30) Ruff, J. K.; Schlientz, W. J. *Inorg. Synth.* **1974**, *15*, 84–90.

(0.417 mmol) of PPNCl was added 25 mL of THF. The solution was stirred at room temperature for 30 min and filtered on a medium frit, and the solvent was removed on a vacuum line. The resultant solid was purified by stirring for a few minutes with 5 mL of benzene, filtering, and then washing several times with 3 mL portions of benzene until these washes were nearly colorless, yielding 0.273 g (73% yield) of product as a black solid. IR (CH₃CN): 1886(s), 1812 (m), 1661 (s) cm⁻¹. ¹H NMR (CD₃CN): δ 7.67–7.44 (m, 37H), 4.62 (s, 6H), 4.33 (s, 5H). ¹³C NMR (CD₃CN): PPN⁺ at δ 134.57 (C₄), 133.22 (quintet, ³J_{PC} = 12 Hz, ⁵J_{PC} = 0 Hz, ²J_{PP} = 7 Hz, C₃), 130.34 (quintet, ²J_{PC} = 13.5 Hz, ⁴J_{PC} = 0 Hz, ²J_{PP} = 7 Hz, C₂), 128.18 (d, ¹J_{PC} = 109.1 Hz, C₁), 93.12 (C₆H₆), 86.83 (Cp). Anal. Calcd for C₅₁H₄₁CrFeP₂NO₄: C, 67.94; H, 4.58; N, 1.55. Found: C, 66.06; H, 4.40; N, 1.57.

Cp(CO)Fe(μ-CO)(μ-COME)Cr(CO)(C₆H₆) (7). A solution of 0.278 g (1.88 mmol) of Me₃OBF₄ dissolved in ~1 mL of CH₃CN was added in one portion to a solution of 0.902 g (1.88 mmol) of **6-Na**⁺·1.3THF in 35 mL of CH₃CN. After the mixture was stirred at room temperature for 5 min, the solvent was removed on a vacuum line; 35 mL of benzene was added to the resultant solid to extract the product, and the solution was filtered through Celite. Following the solvent removal on the vacuum line, the crude product was recrystallized twice from 1:2 CH₂Cl₂/hexane to give 0.205 g (29% yield) of **7** as a black solid. IR(CH₂Cl₂): 1943(s), 1875(m), 1736(m) cm⁻¹. ¹H NMR (CD₂Cl₂, 20 °C): δ 5.31 (C₆H₆), 4.86 (MeO), 4.65 (Cp). ¹H NMR (CD₂Cl₂, -20 °C): δ 5.35, 5.28 (s, 6H, 82:18 cis:trans), 4.89, 4.82 (s, 3H, 18:82 trans:cis), 4.65, 4.59 (s, 5H, 82:18 cis:trans). ¹H NMR (toluene-*d*₈, -20 °C): δ 4.45 (s, 6H), 4.32 (s, 5H), 4.21 (s, 3H) (cis isomer, 59%); δ 4.59(s), 4.58(s) (total 11H), 4.19 (s, 3H) (trans isomer, 41%). ¹³C NMR (CD₂Cl₂, -20 °C): δ 390.41 (carbyne carbon), 286.74 (μ-CO), 236.70 (CrCO, cis), 235.85 (CrCO, trans), 214.87 (FeCO, cis), 214.32 (FeCO, trans), 98.73 (C₆H₆, trans), 97.27 (C₆H₆, cis), 87.87 (Cp, trans), 85.54 (Cp, cis), 71.50 (CH₃). Anal. Calcd for C₁₆H₁₄CrFeO₄: C, 50.82; H, 3.73. Found: C, 49.68; H, 3.55.

¹H NMR Experiments. In the glovebox, solid PPh₃ (for the reactions in which it was used) and 1,4-dichlorobenzene (~6:1 molar ratio to carbyne, added as an internal standard for yield calculations) were loaded into an NMR tube sealed to a 14/20 ground glass joint, while the carbyne was dissolved in a small amount of C₆D₆ and transferred and rinsed into

the tube. C₆D₆ was added to a height of ~5 cm, a vacuum stopcock was fitted to the tube, and the tube was attached to a vacuum line. The tube was submitted to three freeze–pump–thaw cycles and sealed with a torch. The sample was heated in a VWR 1160 water bath at 50.4 ± 0.1 °C and was quenched by immersing in an ice bath. The tube was centrifuged prior to recording each NMR spectrum. The volume was calculated according to the equation $V = \pi(0.205)^2h$, where h is the height of the solvent measured immediately after removal from the hot bath. Each kinetic run was followed for at least 3 half-lives.

The major difficulty was in quantifying the chromium products, since the benzene peaks of (benzene)Cr(CO)₂L (L = CO, PPh₃) overlap precisely at 4.28 ppm in the ¹H NMR spectrum; a 1:1 mixture exhibits this single symmetrical peak in the ¹H NMR spectrum, a single peak in the ³¹P NMR spectrum at 92.39 ppm, and in the ¹³C NMR spectrum benzene peaks in a ~1:1 ratio for (benzene)Cr(CO)₃ (92.33 ppm) and (benzene)Cr(CO)₂PPh₃ (89.40 ppm). Combined yields could be obtained with reasonable confidence, but the relative ratios were determined by comparing the ratio of (benzene)Cr(CO)₂PPh₃ (92.39 ppm) and CpFe(CO)(PPh₃)CH₃ (86.07 ppm) in the ³¹P NMR and then subtracting the derived yield of (benzene)Cr(CO)₂PPh₃ from the combined yield to give the amount of (benzene)Cr(CO)₃. In the control experiment described in the text in which (benzene)Cr(CO)₃ (0.013 M) was heated with PPh₃ (0.40 M; P:Cr = 32:1) at 50 °C for 14 h, ~7.5 ± 1.5% of the mixture was (benzene)Cr(CO)₂PPh₃, as judged by ¹³C NMR.

Acknowledgment. Financial support for this work from the National Science Foundation (Grant Nos. CHE-9096105 for funds for the research and CHE-9408535 for funds for the purchase of the 400 MHz NMR spectrometer) and from the City University of New York Collaborative Incentive Grant Program is gratefully acknowledged.

Supporting Information Available: A table of variable-temperature NMR data (1 page). See any current masthead page for ordering information.

OM970417M